Real-time All-optical Signal Equalisation with Silicon Photonic Recurrent Neural Networks

Ruben Van Assche[(1)], Sarah Masaad[(1)], Emmanuel Gooskens[(1)], Stijn Sackesyn[(1)], Joris Van Kerrebrouck[(1)], Xin Yin[(1)], Peter Bienstman[(1)]

[(1)] Ghent-University/imec, Technologiepark-Zwijnaarde 126, B-9052 Ghent, Belgium, ruben.vanassche@ugent.be

Abstract *We experimentally demonstrate real-time all-optical equalisation of nonlinear fibre distortions using a silicon photonic recurrent neural network. A 28 Gbps OOK signal is equalised with BER below the GFEC threshold* 5.8×10^{-5} *for fibre links up to 50 km. ©2025 The Author(s)*

Introduction

Although originally developed for high-speed, long-distance communication, optical networks are now increasingly utilized in novel applications such as cloud computing and edge services, which involve significant volumes of short-reach traffic within and between data centers. For these short-haul links, intensity-modulation direct-detection (IM/DD) remains the preferred choice due to its lower cost and power requirements compared to coherent transceivers designed for more complex modulation schemes[1]. However, IM/DD systems inherently discard phase information, which imposes limitations on achievable bit-error rates (BER) when contrasted with coherent alternatives. As network demands continue to escalate, improving both the data throughput and power efficiency of IM/DD technologies has become essential. These systems now encounter dual performance bottlenecks: nonlinear signal distortion caused by the optical fiber, and signal degradation from the frequency-dependent response (power fading) of the IM/DD transceivers.

Although digital signal processing techniques can mitigate nonlinear effects, they often come with substantial power consumption and associated costs[2],[3].

To address these issues more efficiently, machine learning approaches—both digital and analog—are gaining traction as promising alternatives[4]–[10].

One promising analog solution involves leveraging photonic neural networks to preprocess optical signals prior to detection. This strategy allows the signal to be conditioned before encountering power fading effects at the receiver, thus avoiding the need for energy-intensive post-detection processing. Notable progress has been made with time-delay based reservoir computing systems and extreme learning machines[11]–[16]. Another emerging technique employs a spatially-distributed reservoir computer, in which a random recurrent neural network processes the input signal, while only the output layer undergoes training. This paper reports, to the best of our knowledge, the first experimental realization of such a system operating in real-time with a fully optical readout[17],[18].

In this study, we developed, fabricated, and experimentally evaluated a spatially-distributed reservoir computing system, applying it to a 28 Gbps on-off keying (OOK) transmission over fiber lengths up to 50 km. We also assessed its performance at launch powers reaching 17 dBm, well into the nonlinear regime. Under these conditions, our system achieves BER values as low as 4×10^{-7}, all comfortably below the standard forward error correction (FEC) threshold of 5.8×10^{-5} commonly employed in Ethernet standards.

Reservoir design

Our photonic reservoir computing (RC) system is fabricated using a Silicon Nitride platform featuring a four-port topology[19]. At each reservoir output, signals emerge as superpositions composed of multiple components with distinct phase shifts and propagation delays. The inherent randomness essential to reservoir function originates from slight fabrication-induced variations, particularly waveguide length differences and surface roughness fluctuations. Consequently, each fabricated chip exhibits a unique yet fixed pattern of random phase shifts across propagating signals. The photodiode at the system output introduces a nonlinear transformation, converting these phase variations between overlapping signals into measurable power fluctuations.

The reservoir architecture incorporates eight nodes, each realized using multimode interferometers (MMIs) interconnected through passive optical waveguides. Figure 1 presents a microscope image highlighting the fabricated photonic chip. A crucial parameter influencing reservoir performance is the length of these interconnecting waveguides, which effectively serve as delay lines. These lengths must be precisely matched to the targeted signal data rate. Numerical simulations

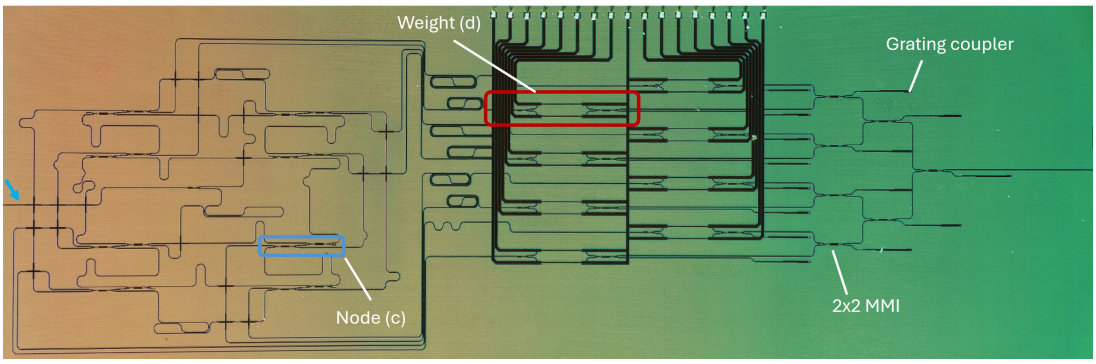

Fig. 1: Design of photonic integrated reservoir (a) Microscope image of the chip design with a blue rectangle showing a node, and a red rectangle showing a weight implemented as an MZI with heaters.

suggest that setting the delay to approximately half of the bit period provides an optimal balance in signal propagation through the reservoir.

The output layer is composed of eight Mach-Zehnder interferometers (MZIs), each directly associated with a reservoir node. Each MZI is individually controlled by two thermo-optic heaters, whose temperatures can be finely adjusted by varying the electrical currents, which in turn will adjust the resulting phase and amplitude of the output signal. This allows the individual reservoir signals to be weighted before they are combined by a summation structure.

Importantly, all reservoir components are passive and linear, substantially simplifying both the fabrication process and operational control. Integration of nonlinear photonic components typically poses significant challenges, either due to the necessity of specialized materials or complex resonance-based control schemes. However, the only source of nonlinearity in our design is the photodiode at the final stage, already inherently required to convert complex optical fields into measurable intensity signals. This nonlinearity turns out to give us enough computational power for the task at hand[20].

Experimental-Set up

The experimental arrangement used in this study is illustrated in Figure 2. Initially, a continuous-wave (CW) laser operating at 1550 nm wavelength undergoes intensity modulation via an on-off keying (OOK) modulator, resulting in an optical data stream at 28 Gbps. Rather than using conventional pseudo-random binary sequence (PRBS) generators, the modulation sequence is generated by the Mersenne Twister algorithm. This approach prevents the reservoir from simply learning the PRBS rule and instead ensures genuine signal equalization capabilities. Distinct initialization seeds are used for the generation of training and testing datasets. Following modulation, the optical signal is amplified by an erbium-doped fiber amplifier (EDFA) to a constant power level of 20 dBm, and subsequently, an adjustable attenuator accurately sets the desired input power without influencing the noise figure of the system.

As the optical signal propagates through the fiber, chromatic dispersion accumulates, causing signal distortion that requires compensation. Due to design and fabrication imperfections, the photonic integrated circuit (PIC) exhibits an insertion loss of approximately 30 dB, necessitating additional amplification. To optimize system performance, amplification is applied both before and after the reservoir. Specifically, EDFA 2 amplifies the input signal up to approximately 15 dBm, while EDFA 3 boosts the reservoir output to a power level of about 10 dBm, suitable for detection by

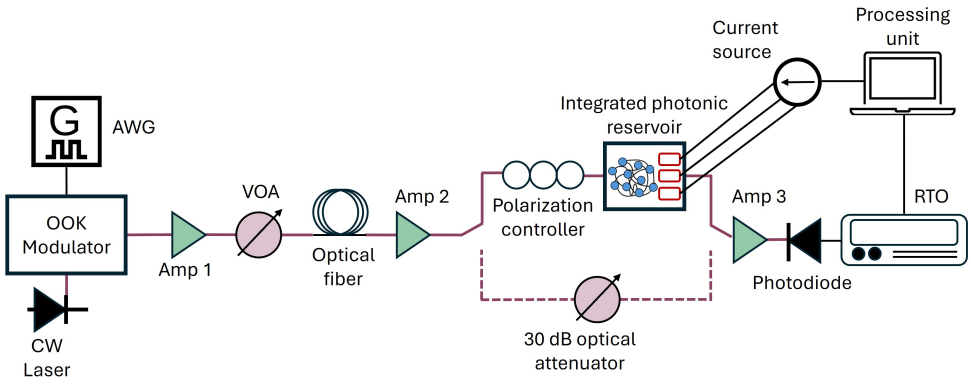

Fig. 2: Experimental set-up The two different setups for the experiments. The upper and lower path respectively show the setup with and without the photonic reservoir. (CW: Continuous wave, AWG: Arbitrary waveform generator, OOK: On-Off keyeing, Amp: Amplifier, RTO: real-time-oscilloscope)

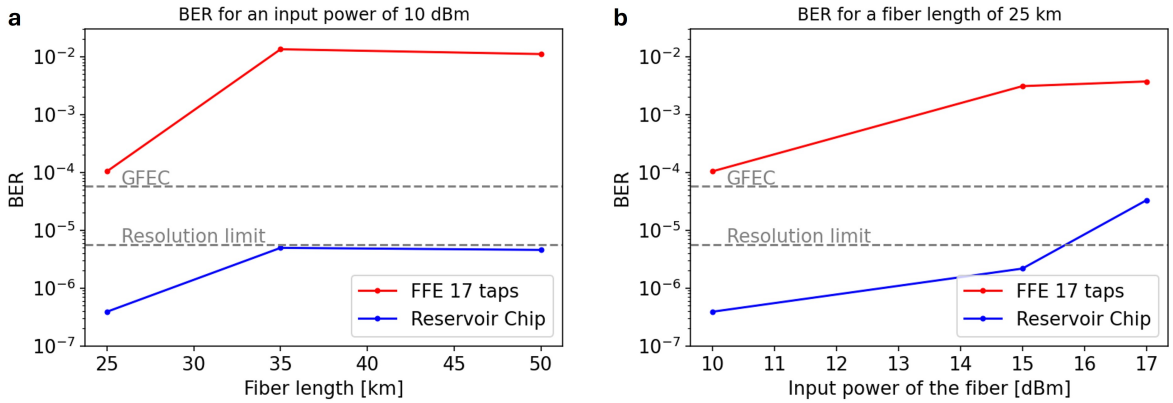

Fig. 3: Experimental bit error rates Measured bit error rates for (a) different lengths of the optical fibre for an input power of 10 dBm and (b) different input powers for a fibre length of 25 km. The grey dashed line signifies the resolution limit up to which predictions can accurately be made for the reservoir, and the GFEC (Generic forward error correction) boundary.

the high-speed photodiode. The electrical current from the photodiode is recorded by a real-time oscilloscope with a sampling rate of 160 GSamples/s. Captured data is processed using an iterative optimization algorithm, which dynamically tunes the electrical currents controlling the PIC's weighting elements, thus establishing a closed-loop optimization cycle.

To facilitate an objective performance evaluation against a conventional electrical feed-forward equalizer (FFE) featuring a tapped delay-line structure, equivalent signal-to-noise ratios (SNRs) must be maintained between both test conditions. This equivalence is achieved by introducing an additional reference path depicted in Figure 2, in which the photonic reservoir is substituted with a fixed 30 dB optical attenuator. This setup preserves identical power levels and removes any influence introduced by the photonic reservoir processing. Additionally, post-processing methods applied to the reservoir output data are exactly replicated for the reference signal path, guaranteeing a fair and unbiased performance comparison between both equalization approaches.

Results

In the experiments, we assessed system performance by sweeping two key parameters: the input optical power launched into the fiber, and the fiber length itself. For a fixed fiber length of 25 km, the input power was varied from 10 to 17 dBm, well within the nonlinear regime. Conversely, to study the effects of propagation distance, we tested fiber spans ranging from 25 to 50 km at a constant launch power of 10 dBm. Extending the fiber length amplifies the cumulative influence of linear and nonlinear dispersion, while higher input power predominantly enhances nonlinear Kerr effects, thereby raising the complexity of the machine learning equalization task.

Figure 3 summarizes the bit-error rate (BER) performance under these varied experimental conditions. Specifically, Figure 3(a) illustrates the evolution of the BER as a function of increasing fiber length, maintaining a constant input power of 10 dBm. In this scenario, chromatic dispersion represents the primary factor limiting signal integrity. As fiber length extends further, performance deteriorates due to the limited memory capacity of both equalization approaches. Remarkably, the photonic reservoir consistently outperforms the feed-forward equalizer (FFE) by at least two orders of magnitude, despite the FFE inherently possessing greater memory. This superior performance arises from the reservoir's richer, nonlinear transformations of the input signal, as opposed to the FFE, which relies solely on linear combinations of delayed replicas of the original signal. Additionally, unlike digital methods, the reservoir operates prior to photodetection, circumventing frequency-dependent power fading issues typically encountered by post-detection digital equalizers.

Figure 3(b) presents BER performance as input power increases, keeping the fiber length fixed at 25 km. In this operating regime, system limitations arise primarily from nonlinear dispersion and its interplay with linear chromatic dispersion effects. Once again, even when matched for the number of adjustable parameters, the photonic reservoir demonstrates a significant improvement in BER performance compared to the FFE, exceeding it by at least two orders of magnitude.

Conclusion

In this work, we experimentally demonstrate a photonic reservoir computing chip capable of equalizing a 28 Gbps on-off keying (OOK) signal well below the generic forward error correction (GFEC) threshold of 5.8×10^{-5} for fibre lengths up to 50 km and input powers up to 17 dBm. Furthermore, we establish the superiority of this approach over a conventional digital feed-forward equalisation (FFE) method, which performs at least two orders of magnitude worse, and it particularly fails in reaching the same GFEC limit.

Acknowledgements

This work was supported by the European Commission in the Horizon Europe programme under the projects Nebula, Prometheus, Neho, and NEHIL.

References

[1] K. Zhong, X. Zhou, J. Huo, C. Yu, C. Lu, and A. P. T. Lau, "Digital signal processing for short-reach optical communications: A review of current technologies and future trends", *Journal of Lightwave Technology*, vol. 36, no. 2, pp. 377–400, 2018. DOI: 10.1109/JLT.2018.2793881.

[2] D. Rafique, J. Zhao, and A. D. Ellis, "Digital back-propagation for spectrally efficient wdm 112 gbit/s pm m-ary qam transmission", *Opt. Express*, vol. 19, no. 6, pp. 5219–5224, 2011. DOI: 10.1364/OE.19.005219. [Online]. Available: https://opg.optica.org/oe/abstract.cfm?URI=oe-19-6-5219.

[3] L. Liu, L. Li, Y. Huang, *et al.*, "Intrachannel nonlinearity compensation by inverse volterra series transfer function", *Journal of Lightwave Technology*, vol. 30, no. 3, pp. 310–316, 2012. DOI: 10.1109/JLT.2011.2182038.

[4] Q. Fan, G. Zhou, T. Gui, C. Lu, and A. P. T. Lau, "Advancing theoretical understanding and practical performance of signal processing for nonlinear optical communications through machine learning", *Nature Communications*, vol. 11, no. 1, p. 3694, 2020.

[5] A. Amari, X. Lin, O. A. Dobre, R. Venkatesan, and A. Alvarado, "A machine learning-based detection technique for optical fiber nonlinearity mitigation", *IEEE Photonics Technology Letters*, vol. 31, no. 8, pp. 627–630, 2019. DOI: 10.1109/LPT.2019.2902973.

[6] X. Pan, X. Wang, B. Tian, C. Wang, H. Zhang, and M. Guizani, "Machine-learning-aided optical fiber communication system", *IEEE Network*, vol. 35, no. 4, pp. 136–142, 2021. DOI: 10.1109/MNET.011.2000676.

[7] C. Häger and H. D. Pfister, "Deep learning of the nonlinear schrödinger equation in fiber-optic communications", in *2018 IEEE International Symposium on Information Theory (ISIT)*, 2018, pp. 1590–1594. DOI: 10.1109/ISIT.2018.8437734.

[8] D. Zibar, M. Piels, R. Jones, and C. G. Schäeffer, "Machine learning techniques in optical communication", *Journal of Lightwave Technology*, vol. 34, no. 6, pp. 1442–1452, 2016. DOI: 10.1109/JLT.2015.2508502.

[9] K. Sozos, F. Da Ros, M. P. Yankov, *et al.*, "Experimental investigation of a recurrent optical spectrum slicing receiver for intensity modulation/direct detection systems using programmable photonics", *Journal of Lightwave Technology*, vol. 42, no. 22, pp. 7807–7815, 2024. DOI: 10.1109/JLT.2024.3430489.

[10] S. Zhang, F. Yaman, K. Nakamura, *et al.*, "Field and lab experimental demonstration of nonlinear impairment compensation using neural networks", *Nature Communications*, vol. 10, no. 1, p. 3033, 2019, ISSN: 2041-1723. DOI: 10.1038/s41467-019-10911-9. [Online]. Available: https://doi.org/10.1038/s41467-019-10911-9.

[11] A. Argyris, J. Cantero, M. Galletero, *et al.*, "Comparison of photonic reservoir computing systems for fiber transmission equalization", *IEEE Journal of Selected Topics in Quantum Electronics*, vol. 26, no. 1, pp. 1–9, 2020. DOI: 10.1109/JSTQE.2019.2936947.

[12] S. M. Ranzini, R. Dischler, F. Da Ros, H. Bülow, and D. Zibar, "Experimental investigation of optoelectronic receiver with reservoir computing in short reach optical fiber communications", *Journal of Lightwave Technology*, vol. 39, no. 8, pp. 2460–2467, 2021. DOI: 10.1109/JLT.2021.3049473.

[13] F. Da Ros, S. M. Ranzini, H. Bülow, and D. Zibar, "Reservoir-computing based equalization with optical pre-processing for short-reach optical transmission", *IEEE Journal of Selected Topics in Quantum Electronics*, vol. 26, no. 5, pp. 1–12, 2020. DOI: 10.1109/JSTQE.2020.2975607.

[14] A. Dejonckheere, F. Duport, A. Smerieri, *et al.*, "All-optical reservoir computer based on saturation of absorption", *Opt. Express*, vol. 22, no. 9, pp. 10 868–10 881, 2014. DOI: 10.1364/OE.22.010868. [Online]. Available: https://opg.optica.org/oe/abstract.cfm?URI=oe-22-9-10868.

[15] Y.-W. Shen, R.-Q. Li, G.-T. Liu, *et al.*, "Deep photonic reservoir computing recurrent network", *Optica*, vol. 10, no. 12, pp. 1745–1751, 2023. DOI: 10.1364/OPTICA.506635. [Online]. Available: https://opg.optica.org/optica/abstract.cfm?URI=optica-10-12-1745.

[16] E. Staffoli, M. Mancinelli, P. Bettotti, and L. Pavesi, "Equalization of a 10gbps imdd signal by a small silicon photonics time delayed neural network", *Photon. Res.*, vol. 11, no. 5, pp. 878–886, 2023. DOI: 10.1364/PRJ.483356. [Online]. Available: https://opg.optica.org/prj/abstract.cfm?URI=prj-11-5-878.

[17] E. Gooskens, S. Sackesyn, J. Dambre, and P. Bienstman, "Experimental results on nonlinear distortion compensation using photonic reservoir computing with a single set of weights for different wavelengths", *Scientific Reports*, vol. 13, no. 1, p. 21 399, 2023.

[18] S. Sackesyn, C. Ma, J. Dambre, and P. Bienstman, "Experimental realization of integrated photonic reservoir computing for nonlinear fiber distortion compensation", *Optics Express*, vol. 29, no. 20, pp. 30 991–30 997, 2021.

[19] S. Sackesyn, C. Ma, J. Dambre, and P. Bienstman, "An enhanced architecture for silicon photonic reservoir computing", 2018. [Online]. Available: https://api.semanticscholar.org/CorpusID:201893967.

[20] K. Vandoorne, P. Mechet, T. Van Vaerenbergh, *et al.*, "Experimental demonstration of reservoir computing on a silicon photonics chip", *Nature Communications*, vol. 5, no. 1, p. 3541, 2014, ISSN: 2041-1723. DOI: 10.1038/ncomms4541. [Online]. Available: https://doi.org/10.1038/ncomms4541.